DOI: https://doi.org/10.5592/CO/EUROENGEO.2024.203

CORRELATION BETWEEN JOINT ROUGHNESS COEFFICIENT (JRC) AND STATISTICAL ROUGHNESS PARAMETERS

NIKIEMA TEGAWENDE [1], GONZE NICOLAS [2], DESCAMPS FANNY [3]

[1] *University of Mons, Belgium, tegawende.nikiema@umons.ac.be*

[2] *University of Mons, Belgium, nicolas.gonze@umons.ac.be*

[3] *University of Mons, Belgium, fanny.descamps@umons.ac.be*

Abstract

Rocks are heterogeneous anisotropic media containing discontinuities that influence their mechanical behavior through their surface morphology, aperture, and filling material. Surface morphology is generally characterized by roughness, which is used as an input parameter in analytical or numerical models of rock mass stability.

Quantifying the roughness of discontinuities is a complex operation that requires appropriate methodologies and tools. Barton's Joint Roughness Coefficient (*JRC*) is widely used due to its simplicity for quantifying roughness and addressing joint shear strength. However, the visual comparison method is subjective and may cause biases in the *JRC* estimates. Several authors proposed to rely on statistical estimators to eliminate such bias.

On this basis, the current study examines the added value of 3D optical profilometry for roughness quantification. Typical *JRC* profiles were digitized, and a 3D printer was used to create surfaces reproducing the roughness state of the profiles. These surfaces were analyzed with a 3D optical profilometer to determine statistical estimators. The most relevant estimators are identified and correlations with the *JRC* are proposed. When investigating the mechanical behavior of rock joints, such correlations will help converting statistical roughness estimates from fractures tested in laboratory into comprehensive *JRC* values to address joint shear strength.

Keywords

Discontinuity, Joint Roughness Coefficient (*JRC*), 3D printed surface, optical profilometer, statistical roughness estimates.

1 Introduction

Rock masses are often crossed by joints that significantly influence their mechanical properties and deformation behavior. Particularly, the shear strength of rock joints depends on their surface irregularities, also called roughness. Barton's empirical criterion (Barton, 1973) obtained from shear tests on various types of rock joints; it is known for estimating rock joints shear strength:

$$\tau = \sigma_n \tan\left[JRC \log_{10}\left(\frac{JCS}{\sigma_n}\right) + \phi_b\right] \quad (1)$$

where τ represents the peak shear stress, σ_n is the effective normal stress, *JRC* is the joint roughness coefficient, *JCS* is the joint compressive strength, and ϕ_b is the basic friction angle. Among those parameters, *JRC* is traditionnally estimated by comparison to standard profiles (Barton & Choubey, 1977). This method is widely used in rock engineering, geotechnics and rock mechanics.

The visual assessment method for *JRC*, however, introduces subjectivity depending on operator's estimation and experience (Hsiung et al., 1993; Beer et al., 2002; Grasselli & Egger, 2003). This has led to an increasing interest in finding more objective and reproducible methods to quantify joint roughness. Methods such as standard profiles digitizing or profilometry allow to compute statistical estimators and led to several correlations (Tse & Cruden, 1979; Maerz et al., 1990; Yu & Vayssade, 1991; Tatone & Grasselli, 2010). Good correlations are generally established with the root mean square slope (Z_2) and the structure function (*SF*). These estimators, while effective, are sensitive to sampling intervals, introducing variability in relationships (Yu & Vayssade, 1991). Other correlations involving fractal dimensions have been explored, but deriving distinctive fractal dimensions for roughness profiles with self-affine characteristics remains challenging (Huang et al., 1992; Li & Huang, 2015).

In the current study, two methods are proposed to analyze *JRC* profiles. The first method is the digitization of profiles in order to analyze them in terms of statistical estimators. The second method deals with optical profilometry on 3D printed profiles in order to automate fracture roughness quantification for laboratory samples. Results are compared to literature data to validate the proposed methodologies.

2 Methods

Barton & Choubey (1977) used a comb with a set of teeth estimated at 1 mm diameter over a length of 10 cm to fit the joint surface and draw the corresponding 2D roughness profile. A total of 136 rock joint surface specimens were profiled, in most cases 3 profiles per surface, to obtain the ten standard profiles. The *JRC* values obtained by back-calculation were classified in intervals of two from 0 (lowest roughness) to 20 (highest roughness).

Several parameters have been used by other authors (Tse & Cruden, 1979; Maerz et al., 1990; Yu & Vayssade, 1991; Hsiung et al., 1993; Tatone & Grasselli, 2010; Jang et al., 2014) and the most common are considered in this study: the root means square slope (Z_2), the structure function (SF) and the linear roughness (R_L) or roughness profile index (R_p). They are defined as follows:

$$Z_2 = \left[\frac{1}{L}\int_0^L \left(\frac{dz}{dx}\right)^2 dx\right]^{1/2} \approx \left[\frac{1}{N-1}\sum_{i=1}^{N-1}\left(\frac{z(x_{i+1})-z(x_i)}{x_{i+1}-x_i}\right)^2\right]^{1/2} \quad (2)$$

$$SF = \frac{1}{L}\int_0^L [z(x_{i+1})-z(x_i)]^2 dx \approx \frac{1}{N-1}\sum_{i=1}^{N-1}(z_i - z_{i+1})^2 \quad (3)$$

$$R_P = \frac{\sum_{i=1}^{N-1}[(z_{i+1}-z_i)^2 - (x_{i+1}-x_i)^2]^{1/2}}{L} \quad (4)$$

where L is the length of the profile, z is the height of the profile, x is the x-coordinate, N is the number of z differential points.

2.1 Digitization of standard *JRC* profiles

Several steps are required to analyse the *JRC* profiles in terms of statistical estimators. First of all, the ten standard profiles (ISRM, 1978) were scanned with a 100dpi resolution, providing images with 440 pixels for 10 cm and a pixel size of 0.227 mm. This resolution is chosen to comply with the physical roughness determination from profile combs (1mm diameter teeth on a 10 cm length). Every image file is saved in black and white format. A Python code was developed for digitizing the images. X-coordinates are taken at the center of each pixel, while y-coordinates are computed as the median of all

black pixels corresponding to a given x-value (Figure 1). Then, the roughness profile is shaped by linking consecutive points by a linear segment. Other researchers also digitized standard *JRC* profiles with different methodologies and sampling intervals. Their work is summarised in Table 1.

Standard profiles have different horizontal lengths. This observation is similar to that made by Jang et al. (2014). The 7th profile (*JRC 12–14*) is the shortest (95.89 mm) and the 8th profile (*JRC* 14–16) is the longest (100.10 mm). In addition, they are not horizontal, i.e. their reference best-fit straight line is not horizontal (Tatone & Grasselli, 2010) and a rotation is performed in order to align the best-fit line with the horizontal axis. Figure 2 shows the digitized *JRC* 14–16 profile (original profile) and the corresponding one after rotation. After that, a Python code was used to compute roughness estimators for different sampling intervals. The value of each interval was determined from the highest point in the interval to simulate the use of a Barton's comb.

Table 1. Some *JRC* digitizing methods and proposed correlations with statistical estimators.

Digitizing method	Sampling interval [mm]	Proposed correlation	R^2	Reference
Profile enlarged 2.5 x X-sampling = 1.27 mm Y-sampling = smooth curve Reference line = mean of all the amplitudes	1.27	$JRC = 32.47log(Z_2) + 32.20$	0.986	Tse & Cruden (1979)
		$JRC = 16.58log(SF) + 37.28$	0.984	
Shadow profilometry X-sampling 0.20 mm Y-sampling = center line	0.50	$JRC = 411(R_P - 1)$	0.984	Maerz and al. (1990)
		$JRC = 401(R_P - 1)$	0.973	
Philips digital A3 plotter Profile enlarged 2.4 x X-coordinates 0.6, 1.2 and 2.4 mm Y-sampling = center line	0.25	$JRC = 60.32(Z_2) - 4.51$	0.968	Yu & Vayssade (1991)
		$JRC = 239.27(\sqrt{SF}) - 4.51$	0.968	
		$JRC = 558.68(R_P) - 557.13$	0.951	
	0.50	$JRC = 61.79(Z_2) - 3.47$	0.973	
		$JRC = 121.13(\sqrt{SF}) - 3.28$	0.972	
		$JRC = 559.73(R_P) - 597.46$	0.974	
	1.00	$JRC = 64.22(Z_2) - 2.31$	0.983	
		$JRC = 63.69(\sqrt{SF}) - 2.31$	0.983	
		$JRC = 702.67(R_P) - 699.99$	0.951	
AutoCAD Scanned image in black and white at 1 200 dpi X-sampling: 0.5 mm Y-sampling: manual Reference line = fit-line of all the amplitudes	0.50	$JRC = 51.85(Z_2)^{0.60} - 10.37$	0.960	Tatone & Grasselli (2010)
		$JRC = \left[3.36x10^{-2} + \frac{1.27x10^{-3}}{\ln(R_P)}\right]^{-1}$	0.972	
	1.00	$JRC = 55.03(Z_2)^{0.74} - 6.10$	0.977	
		$JRC = \left[3.38x10^{-2} + \frac{1.07x10^{-3}}{\ln(R_P)}\right]^{-1}$	0.972	
Origine software Scan image at 1 200 dpi (black and white) X-sampling: 0.1, 0.5, 1.0 and 2.0 mm Y-sampling: center line	0.50	$JRC = 51.16(Z_2)^{0.531} - 11.44$	0.972	Jang et al. (2014)
		$JRC = 73.95(SF)^{0.226} - 11.38$	0.972	
		$JRC = 65.9(R_P - 1)^{0.302} - 9.61$	0.973	

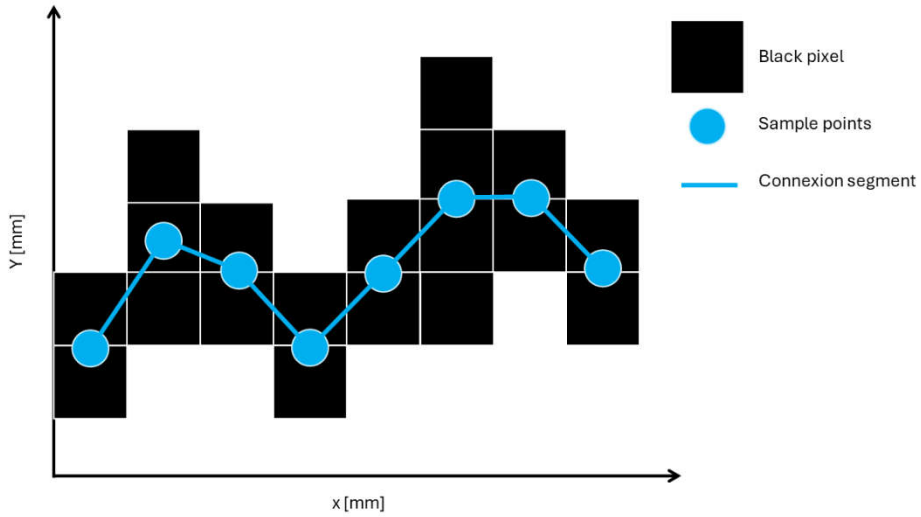

Figure 1. Illustration of the digitization methodology.

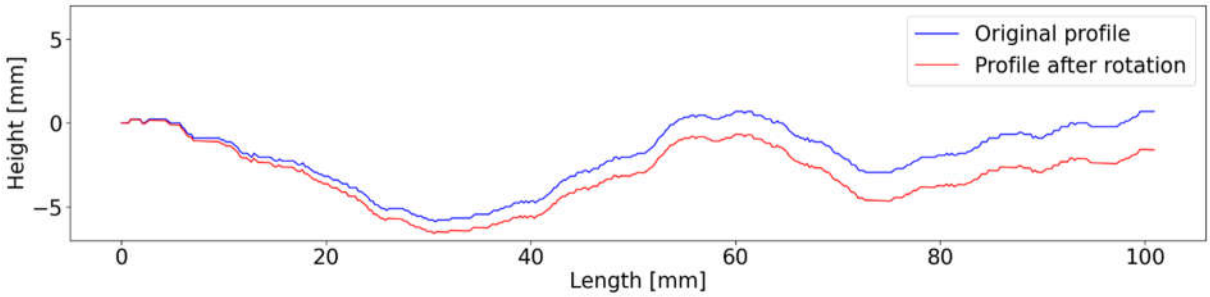

Figure 2. Digitized *JRC* 14-16 profile in its original orientation (blue) and after rotation (red).

2.2 Three-dimensional printing and profilometry

The ten digitized profiles were also printed as 3D surfaces by Elegoo Mars 3 resin printing device, with a resolution of 10 µm in z and 0.035 µm in x and y.

The 3D optical profilometer Keyence VR-6200 has been used to scan the 3D printed surfaces. The profilometer has a resolution of ± 4 µm in z and ±5 µm in x and y directions. It uses optics to create linear fringe projection light through built-in high intensity light-emitting diodes (LED). The light impinges the object diagonally with a precise angle. When there are height differences on the surface of the object, the fringe projection image is distorted in relation to the height difference of the object. The distorted fringe projection image is captured by complementary metal–oxide–semiconductor (CMOS) monochrome cameras from straight above, and the object height is measured from the distortion. When there are no height differences on the impinge surface, the fringe projection light remains undistorted. The profilometer applies the light from both right and left projection units to minimize the influence of the object's shape and orientation. An example of a 3D printed surface and a 3D scanned surface is shown in Figure 3.

The analysis module provided with the profilometer proposes more than 30 statistical estimators, most of them proposed in ISO 4287 (1997), which were examined to look for relation with the *JRC*. These estimators can be determined either from raw measured data or using the stylus mode. The purpose of this mode is to mimic the operation of a mechanical profilometer by simulating the displacement of a stylus along the profile to analyze. This mode enables the user to change the tip radius (from 1 to 500 µm) and the tip angle (from 1 to 120°) of the stylus. Increasing the radius, as discussed below, has the effect of smoothing the profile and eliminating minor vertical variations.

In this study, in order to compare methodologies, Z_2 and R_P are considered. The raw data profiles were also processed by the Python code developed for the scanned profiles to compare and validate the different approaches (Barton's comb and stylus mode).

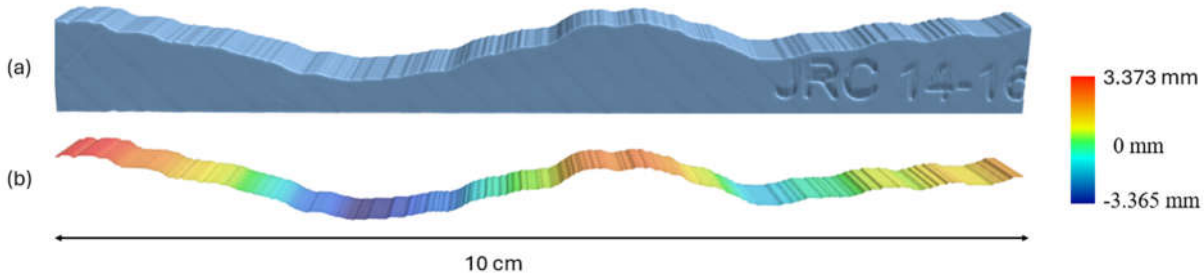

Figure 3. Illustration of 3D printed *JRC* 14-16 profile (a) and the corresponding scanned profile (b).

3 Results

First, the dependency on the sampling interval is investigated. All the estimators vary according to the sampling interval, as illustrated for Z_2 (Figure 4a) and R_P (Figure 4b). The variation is non-linear and statistical estimators tend to decrease when the sampling interval increases. The influence of the sampling interval decreases significantly as the interval increases, and becomes negligible for an interval close to 1 mm. The values of *JRC* 6–8 are similar to those of *JRC* 8-10.

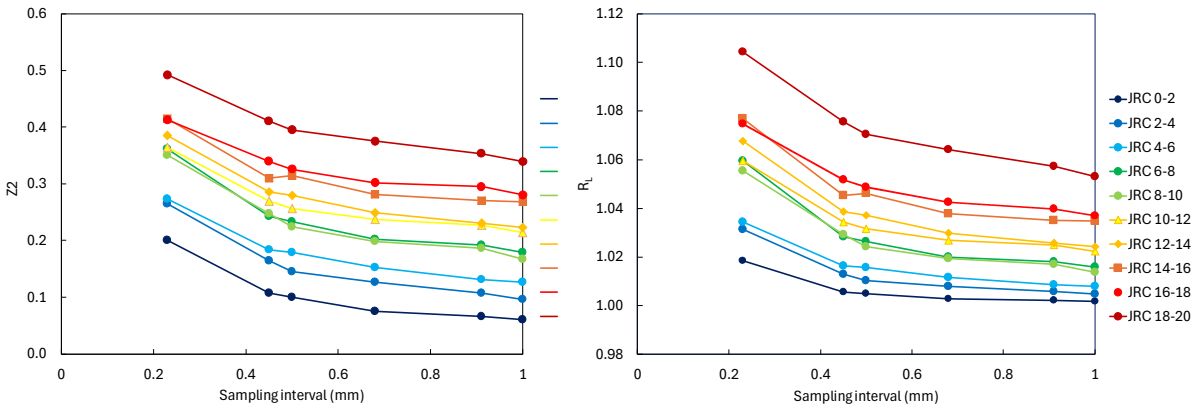

Figure 4. Influence of sampling interval on statistical estimators of JRC. (a) Z_2. (b) R_P.

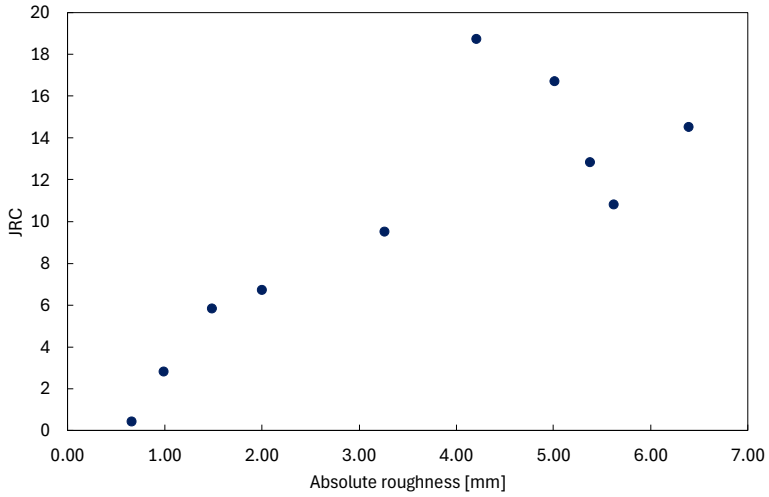

Figure 5. Absolute roughness of the standard *JRC* profiles.

The parameters that do not consider the differential of the amplitude z (e.g. absolute roughness, arithmetic roughness) are poorly correlated with *JRC*. We observe that the absolute roughness of the *JRC* 12–14, *JRC* 16–18, and *JRC* 18–20 profiles is smaller than those of the immediately preceding profiles (Figure 5).

In agreement with the geometry of profile combs and as proposed by many authors, sampling intervals of 0.5 mm and 1.0 mm are considered for further analysis of roughness estimates. In stylus mode, stylus diameters of 0.5 and 1.0 mm respectively are considered.

Z_2 is probably the most used estimator for *JRC* (Tse & Cruden, 1979; Yu & Vayssade, 1991; Tatone & Grasselli, 2010). The relationship between *JRC* and Z_2 is illustrated in Figure 6a and b. Z_2 estimated from digitized profiles and from profilometry give consistent results and are also very close to previously published data. For a 1.0 mm sampling interval, data from both methods even overlap each other. On those graphs, Z_2 is also obtained from the stylus mode of the profilometer. In this case, data are shifted to the right. The offset is about 0.1 for all profiles and whatever the sampling interval and can be explained by the implementation of the stylus mode on the profilometer which does not reproduce the physical principle of a profile comb. Linear correlations are proposed between Z_2 and *JRC* (Table 2).

Similarly, *JRC* vs R_P plots are proposed in Figure 6c and d. Again, R_P computed from digitized profiles and from profilometer are consistent with literature data and overlap on Figure 6d. R_P is linearly correlated with JRC (Table 2). The stylus method gives slightly different results and, in this case, the regression lines are not parallel to the others.

SF is addressed in Figure 6e and f. This statistical estimator has not been used by many authors and literature data show some discrepancy. Our results fit quite well with Yu & Vayssade's ones (1991). Similary to them, we observe a linear correlation between $\sqrt{SF}$ and *JRC*. For the digitized and the profilometric calculating method, the regression curves are close to each other when the sampling interval is 0.50 mm, and they even overlap when the sampling interval is 1.00 mm.

Table 2. Correlation equation between JRC and Z_2, SF and R_p for sampling intervals 0.50 mm and 1.00 mm.

	Sampling interval = 0.50 mm		Sampling interval = 1.00 mm	
Methodology	Correlation	R^2	Correlation	R^2
Digitized profiles	$JRC = 66.20Z_2 - 6.38$	0.966	$JRC = 67.49Z_2 - 3.32$	0.967
	$JRC = 132.06\sqrt{SF} - 6.376$	0.966	$JRC = 67.154\sqrt{SF} - 3.324$	0.967
	$JRC = 290.7R_P - 290$	0.932	$JRC = 354(R_P) - 351.75$	0.919
Optical profilometer	$JRC = 64.79Z_2 - 5.09$	0.966	$JRC = 66.14Z_2 - 2.93$	0.967
	$JRC = 129.59\sqrt{SF} - 5.091$	0.966	$JRC = 66.138\sqrt{SF} - 2.927$	0.967
	$JRC = 302.18\,R_P - 300.86$	0.924	$JRC = 349.27R_P - 346.76$	0.908
Optical profilometer (Stylus mode)	$JRC = 65.25Z_2 - 11.21$	0.935	$JRC = 64.87Z_2 - 9.36$	0.949
	$JRC = 238.6R_P - 240.57$	0.924	$JRC = 248.38R_P - 249.39$	0.929

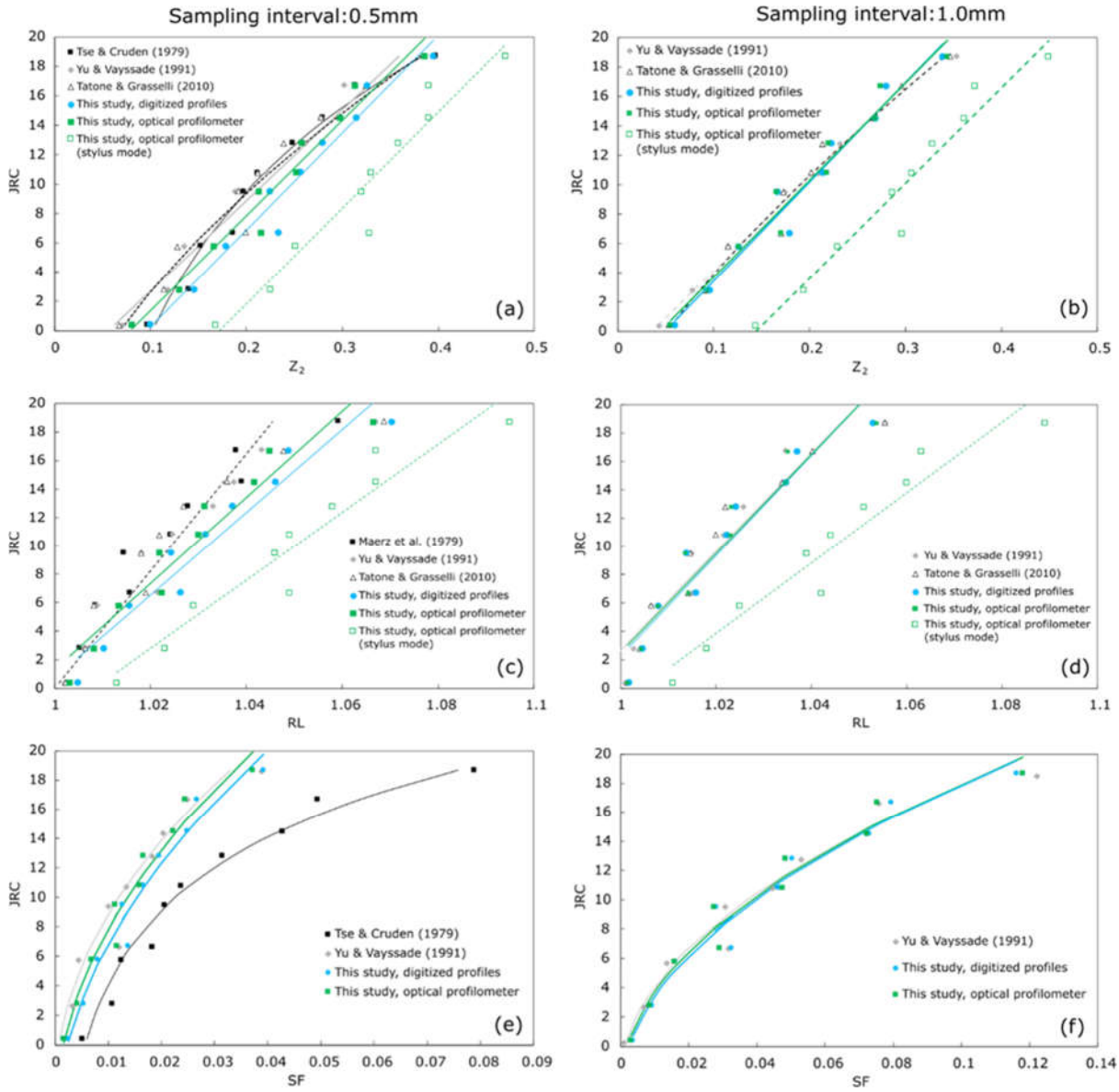

Figure 6. Relationships between statistical estimators and *JRC* for sampling intervals of 0.5mm (a, c and e) and 1.0mm (b, d and f). Estimators are computed from digitized profiles (blue dots) and from profilometry (green squares). For profilometry, stylus mode values are also considered when available (Z_2 and R_P only).

4 Conclusion

This study addresses the quantification of joint roughness using advanced methodologies to overcome the subjectivity and enhance the reproducibility of the *JRC* estimation. The ten Barton' standard profiles have been digitized, printed into 3D surfaces and scanned with an optical profilometer. The most common statistical estimators (Z_2, R_P and *SF*) have been calculated in order to explore for correlation with *JRC*. Our results generally fit with the ones proposed in literature (Tse & Cruden, 1979; Yu & Vayssade, 1991; Tatone & Grasselli, 2010; Maerz et al. 1990). For Z_2 and R_P, a stylus mode is available with profilometric measurement. This method gives slightly different results but the data are still well correlated with *JRC*. In future work on geometric characterization of fracture roughness, such statistical estimates from profilometer can be considered as an efficient tool for automated description of laboratory fracture surfaces.

References

Barton, N. Review of a new shear-strength criterion for rock joints. *Engineering Geology*. 1973, *7* (4), 287–332. DOI: 10.1016/0013-7952(73)90013-6

Barton, N., & Choubey, V. The shear strength of rock joints in theory and practice. *Rock Mechanics Felsmechanik Mécanique Des Roches*. 1977, *10* (1–2), 1–54. DOI: 10.1007/BF01261801

Beer, A. J., Stead, D., & Coggan, J. S. Technical Note Estimation of the Joint Roughness Coefficient (JRC) by Visual Comparison. *Rock Mechanics and Rock Engineering*. 2002, *35* (1), 65–74. DOI: 10.1007/s006030200009

Grasselli, G., & Egger, P. Constitutive law for the shear strength of rock joints based on three-dimensional surface parameters. *International Journal of Rock Mechanics and Mining Sciences*. 2003, *40* (1), 25–40. DOI: 10.1016/S1365-1609(02)00101-6

Hsiung, S. M., Ghosh, A., Ahola, M. P., & Chowdhury, A. H. Assessment of conventional methodologies for joint roughness coefficient determination. *International Journal of Rock Mechanics and Mining Sciences & Geomechanics Abstracts*. 1993, *30* (7), 825–829. DOI: 10.1016/0148-9062(93)90030-H

Huang, S. L., Oelfke, S. M., & Speck, R. C. Applicability of fractal characterization and modelling to rock joint profiles. *International Journal of Rock Mechanics and Mining Sciences & Geomechanics Abstracts*. 1992, *29* (2), 89–98. DOI: 10.1016/0148-9062(92)92120-2

ISO 4287. *Geometrical Product Specifications (GPS) - Surface texture: Profile method - Terms, definitions and surface texture parameters*. 1997

ISRM. *Suggested methods for the quantitative description of discontinuities in rock masses*. 1978.

Jang, H. S., Kang, S. S., & Jang, B. A. Determination of Joint Roughness Coefficients Using Roughness Parameters. *Rock Mechanics and Rock Engineering*. 2014, *47* (6), 2061–2073. DOI: 10.1007/s00603-013-0535-z

Li, Y., & Huang, R. Relationship between joint roughness coefficient and fractal dimension of rock fracture surfaces. *International Journal of Rock Mechanics and Mining Sciences*. 2015, *75* , 15–22. DOI: 10.1016/j.ijrmms.2015.01.007

Maerz, N. H., Franklin, J. A., & Bennett, C. P. Joint roughness measurement using shadow profilometry. *International Journal of Rock Mechanics and Mining Sciences & Geomechanics Abstracts*. 1990, *27* (5), 329–343. DOI: 10.1016/0148-9062(90)92708-M

Tatone, B. S. A., & Grasselli, G. A new 2D discontinuity roughness parameter and its correlation with JRC. *International Journal of Rock Mechanics and Mining Sciences*. 2010, *47* (8), 1391–1400. DOI: 10.1016/j.ijrmms.2010.06.006

Tse, R., & Cruden, D. M. Estimating joint roughness coefficients. *International Journal of Rock Mechanics and Mining Sciences & Geomechanics Abstracts*. 1979, *16* (5), 303–307. DOI: 10.1016/0148-9062(79)90241-9

Yu, X., & Vayssade, B. Joint profiles and their roughness parameters. *International Journal of Rock Mechanics and Mining Sciences & Geomechanics Abstracts*. 1991, *28* (4), 333–336. DOI: 10.1016/0148-9062(91)90598-G